arXiv:1512.06251v1 [cond-mat.stat-mech] 19 Dec 2015

Coherent response of a stochastic nonlinear oscillator to a driving force: analytical characterization of the spectral signatures

J. Plata

Departamento de Física, Universidad de La Laguna,

La Laguna E38204, Tenerife, Spain.

Abstract

We study the dynamics of a classical nonlinear oscillator subject to noise and driven by a sinusoidal force. In particular, we give an analytical identification of the mechanisms responsible for the supernarrow peaks observed recently in the spectrum of a mechanical realization of the system. Our approach, based on the application of averaging techniques, simulates standard detection schemes used in practice. The spectral peaks, detected in a range of parameters corresponding to the existence of two attractors in the deterministic system, are traced to characteristics already present in the linearized stochastic equations. It is found that, for specific variations of the parameters, the characteristic frequencies near the attractors converge on the driving frequency, and, as a consequence, the widths of the peaks in the spectrum are significantly reduced. The implications of the study to the control of the observed coherent response of the system are discussed.

PACS numbers: 05.40.Ca, 05.45. a, 89.75.Da

I. INTRODUCTION

The combined effect of noise and deterministic driving can lead to a variety of nontrivial features in the dynamics of nonlinear systems [1]. Remarkable effects emerging in different variations of this scenario are stochastic resonance [2], noise-induced transport [3], stochastic phase-switching [4–6], and synchronization [7, 8]. The interest of the characterization of novel phenomenology in these systems is clear: the combination of their fundamental components (i.e., nonlinearity, driving forces, and fluctuations) can be relevant to widely different contexts. (See [9, 10] for recent developments in this field.) Here, we focus on an effect detected in a recent realization of a basic model [11]. Namely, we concentrate on the supernarrow peaks observed in the spectrum of a nonlinear micro-mechanical torsional oscillator driven by a sinusoidal force and subject to broadband noise of controllable intensity. Apart from the standard δ-component at the driving frequency, (associated with the *deterministic* component of the output), the spectral density was found to display nontrivial supernarrow peaks emerging from the (continuous) noisy background. Those peaks appeared at the driving frequency, (for specific values of it), presented an asymmetric form, and widened for increasing noise intensities. Secondary maxima were also detected. The presence of those features was found to coincide with the occurrence of approximately equal populations in the two attractors existent in the system at the considered frequency values. (The term *supernarrow peak* used along the paper is understood as it is defined in [12]: it refers to a peak whose width is much smaller than the inverse of the relaxation time.) Here, we intend to evaluate the connection of those effects with particular aspects of the deterministic dynamics. In order to analytically establish that link, we concentrate on a range of parameters where the nonlinear term can be considered as a perturbation. In that regime, we present a description of the dynamics based on averaging techniques applicable to stochastic systems. From our approach, the mechanism responsible for the detected behavior is uncovered and the elements of the system which are essential for the appearance of the observed features are identified. Furthermore, our semi-analytical picture of the dynamics provides us with some clues to controlling the system response. The direct implications of the study to the implementation of techniques of stabilization of the system are evident. Additionally, because of the fundamental character of the physics involved, the analysis can be relevant to diverse contexts, where conditions similar to those realized in the

basic scenario can be implemented. Here, it is worth pointing out the existence of previous interesting work on related systems [12, 13]. In [12], an analytical approach to the spectral density was presented; in [13], the activation energy between attractors in the configuration space was evaluated. In our approach, a set of variables directly related to those measured in the experiments is used. Moreover, we explicitly apply the averaging methods that parallel the practical techniques.

The outline of the paper is as follows. In Sec. II, we present our approach to the noisy dynamics of a damped and driven nonlinear oscillator. Through the application of the averaging methods of Bogoliubov, Krylov, and Stratonovich [14, 15], we derive an effective description in terms of a system of stochastic differential equations for the amplitude and the phase. In Sec. III, the validity of our approach is confirmed through the qualitative simulation of the main experimental findings. Moreover, we obtain the spectrum for a linearized version of the model; from it, crucial aspects of the role of noise in the response of the system to the driving are identified. Finally, some general conclusions are summarized in Sec. IV.

II. THE MODEL SYSTEM

We consider a damped nonlinear oscillator driven by a sinusoidal force and under the effect of additive noise. Specifically, we assume that the evolution of the position coordinate z (normalized to a typical system length, and, therefore, dimensionless) is described by the equation

$$\ddot{z} = -2\gamma\dot{z} - \omega_0^2 z + \beta z^3 + E\sin(\omega_d t) + \zeta(t), \tag{1}$$

where the potential is characterized by the basic frequency ω_0 and the nonlinear coefficient $\beta\,(>0)$. (Residual anharmonic terms present in the experimental setup are not included as they were shown to play no significant role in the detected features [11].) Additionally, γ is the friction coefficient, E and ω_d respectively stand for the amplitude and frequency of the driving field, and $\zeta(t)$ denotes the stochastic force. In order to simulate the experimental realization, $\zeta(t)$ is modeled as general Gaussian wideband noise [16]: the correlation function, $k_\zeta(t'-t) \equiv \langle\zeta(t)\zeta(t')\rangle - \langle\zeta(t)\rangle^2$, is assumed to have a generic functional form, and the correlation time is considered to be much shorter than any other relevant time scale in the

system evolution. The intensity coefficient $D = \frac{1}{2}\int_{-\infty}^{\infty} k_\zeta(\tau)d\tau$ will be used to characterize the noise strength [15]. (The white-noise limit, defined by $k_\zeta(t'-t) = 2D\delta(t-t')$, is included in the analysis.) Additionally, a zero mean value, $\langle\zeta(t)\rangle = 0$, is considered. (A nonzero $\langle\zeta(t)\rangle$ can be simply incorporated into the model as an effective deterministic contribution.)

A. The averaging method

Our approach to deal with Eq. (1) is based on the coarse-graining techniques developed by Krylov and Bogoliubov for the analysis of deterministic nonlinear oscillations as they were adapted by Stratonovich to the study of stochastic processes [14, 15]. Those averaging methods can be applied to generic wideband fluctuations with sufficiently short correlation time. In this approach, the amplitude A and the phase Ψ of the oscillations are defined through the equations

$$\begin{aligned} z &= A\cos(\omega_d t + \Psi) \\ \dot{z} &= -\omega_d A\sin(\omega_d t + \Psi) \end{aligned} \tag{2}$$

With these changes, Eq. (1) is reduced to a system of two first-order equations in *standard form* [15, 17], i.e., with a structure corresponding to a harmonic oscillator perturbed by deterministic and stochastic terms. For $\omega_d \gg \gamma$, the average of the deterministic perturbative elements over the period $\tau_d = 2\pi/\omega_d$ is readily carried out. Moreover, for a noise correlation time much smaller than the relaxation times of the amplitude and the phase, the coarse graining of the stochastic terms over τ_d can be applied following the procedure presented in [15]. Accordingly, we obtain that, to first order, the averaged equations are [15, 17]

$$\dot{A} = -\gamma A - \frac{1}{2}\frac{E}{\omega_d}\cos\Psi + \frac{1}{4}\frac{D_{eff}}{\omega_d}\frac{1}{A} + \xi_1(t), \tag{3}$$

$$\dot{\Psi} = \Delta - \frac{3}{8}\frac{\beta}{\omega_d}A^2 + \frac{1}{2}\frac{E}{\omega_d}\frac{1}{A}\sin\Psi + \frac{\xi_2(t)}{A}, \tag{4}$$

where we have incorporated the detuning $\Delta = \omega_0 - \omega_d$ and have assumed that $\omega_0 + \omega_d \simeq 2\omega_d$. $\xi_1(t)$ and $\xi_2(t)$ are effective Gaussian white-noise terms defined by $\langle\xi_i(t)\rangle = 0$ and $\langle\xi_i(t)\xi_j(t')\rangle = 2D_{eff}\delta_{i,j}\delta(t-t')$, $(i,j = 1,2)$, with $D_{eff} = \kappa_\zeta(\omega_d)/(4\omega^2)$. [$D_{eff}$, which determines the strength of the (uncorrelated) effective noise terms, is obtained from the

power spectral density $\kappa_\zeta(\omega) \equiv \int_{-\infty}^{\infty} e^{i\omega\tau} k_\zeta(\tau) d\tau$ of the original noise $\zeta(t)$ at the frequency ω_d. From the broadband characteristics assumed for $\zeta(t)$, a smooth form of $\kappa_\zeta(\omega)$ can be inferred. Indeed, a completely flat spectrum occurs in the white-noise limit.] Whereas the noise term in Eq. (3), $\xi_1(t)$, is additive, the fluctuations enter Eq. (4) through the term $\xi_2(t)/A$, and, therefore, have multiplicative character. Moreover, it is important to take into account the presence of the noise-induced *deterministic* term $\frac{1}{4}\frac{D_{eff}}{\omega_d}\frac{1}{A}$ in Eq. (3). Because of this term, the point defined by $A = 0$ is never reached in the stochastic dynamics. (We stress that the emergence of this term is due to the multiplicative character of noise in the set of variables corresponding to the amplitude and phase [15].) The use of averaged equations is specially appropriate for the considered experimental setup: the specific characteristics of the applied detection scheme imply that the registered data do actually correspond to averaged magnitudes. (Equations with a similar form have been extensively studied by Stratonovich in the context of nonlinear self-excited oscillations in electronic circuits [15].)

B. The deterministic dynamics

In order to trace the response of the system to noise, we must clearly define the deterministic scenario into which the fluctuations enter. (See [18] for an exhaustive presentation of standard techniques applicable to this context.) The noiseless dynamics is described by Eq. (1) without the random term $\zeta(t)$, and, consequently, by Eqs. (3) and (4) with $D_{eff} = 0$. The stationary values of the amplitude A_s and phase Ψ_s are obtained by setting $\dot{A} = 0$, and $\dot{\Psi} = 0$ in Eqs. (3) and (4). After minor algebra, it is found that A_s is obtained from the roots x_s of the equation

$$(1 - x)^2 x = c_1 - c_2 x \tag{5}$$

where we have introduced the coefficients $c_1 = \frac{3}{32}\frac{E^2\beta}{\omega_d^3\Delta^3}$, and $c_2 = -\frac{\gamma^2}{\Delta^2}$, and have scaled the squared amplitude as $x = \frac{3}{8}\frac{\beta}{\omega_d\Delta}A^2$. Additionally, the stationary phase Ψ_s is given by

$$\tan\Psi_s = \frac{\Delta}{\gamma}(1 - x_s) \tag{6}$$

The graphical resolution of Eq. (5) is illustrated in Fig. 1 for different values of the driving frequency. The fixed points correspond to the intersections between the graphics of the functions $f(x) \equiv (1 - x)^2 x$ and $g(x) \equiv c_1 - c_2 x$. Their number, localization, and stability

are strongly dependent on ω_d, which enters the coefficients c_1, c_2, and the scaling factor $\frac{x}{A^2} = \frac{3}{8}\frac{\beta}{\omega_d \Delta}$, directly, and/or, through the detuning. Let us look at the stability. The analysis of the linearized equations is straightforward: taking $A = A_s + \delta A$, and $\Psi = \Psi_s + \delta\Psi$, and defining $u \equiv \delta A$ and $v \equiv A_s \delta\Psi$, we find

$$\dot{u} = -\eta_1 u + \lambda_1 v, \tag{7}$$

$$\dot{v} = \lambda_2 u - \eta_2 v. \tag{8}$$

where the diagonal elements read $\eta_1 = \eta_2 = \gamma$, and the coupling terms are

$$\begin{aligned} \lambda_1 &= \Delta(x_s - 1) \\ \lambda_2 &= \Delta(1 - 3x_s). \end{aligned} \tag{9}$$

The characteristic frequencies $\Omega_\pm$ are trivially given by the expression

$$\Omega_\pm = \frac{1}{2}\left[-(\eta_1 + \eta_2) \pm \sqrt{(\eta_1 - \eta_2)^2 + 4\lambda_1\lambda_2}\right], \tag{10}$$

which for the considered parameters becomes

$$\Omega_\pm = -\gamma \pm \Delta\sqrt{(x_s - 1)(1 - 3x_s)}. \tag{11}$$

Then, the time evolution is given by $u(t) = G_+ e^{\Omega_+ t} + G_- e^{\Omega_- t}$, and by a similar equation for $v(t)$. (G_+ and G_- are constants determined by the initial conditions.) Moreover, for the original system, connected with its coarse-grained reduction through the change of variables introduced in Eq. (2), we can write

$$\begin{aligned} z(t) &= (A_s + u)\cos(\omega_d t + \Psi_s + \frac{v}{A_s}) \\ &\approx A_s \cos(\omega_d t + \Psi_s) + u\cos(\omega_d t + \Psi_s) - v\sin(\omega_d t + \Psi_s). \end{aligned} \tag{12}$$

Therefore, apart from a constant-amplitude oscillation with frequency ω_d, $z(t)$ incorporates two terms with time-dependent amplitudes $u(t)$ and $v(t)$. In a generic regime, since the frequencies $\Omega_\pm$ can be complex, the global output signal can have contributions centered at

frequencies shifted from ω_d, coming from the modulation terms. In the particular regimes where the frequencies $\Omega_\pm$ take negative real values, the modulated oscillations are merely damped signals at the external frequency. The precise identification of the different regimes will be crucial for explaining the coherent response of the stochastic system to the driving.

From Eq. (10), it is apparent that necessary and sufficient conditions for stability, i.e., for both frequencies to have negative real parts, (and, consequently, for the solutions to decay in time), are

$$\eta_1 + \eta_2 > 0, \tag{13}$$

and

$$\eta_1\eta_2 - \lambda_1\lambda_2 > 0. \tag{14}$$

For the parameters of our system, Eq. (13) trivially holds and Eq. (14) is cast into

$$\gamma^2 - \Delta^2(x_s - 1)(1 - 3x_s) > 0. \tag{15}$$

As the driving frequency is varied, Δ and x_s are modified, and, in turn, the stability of the sa-

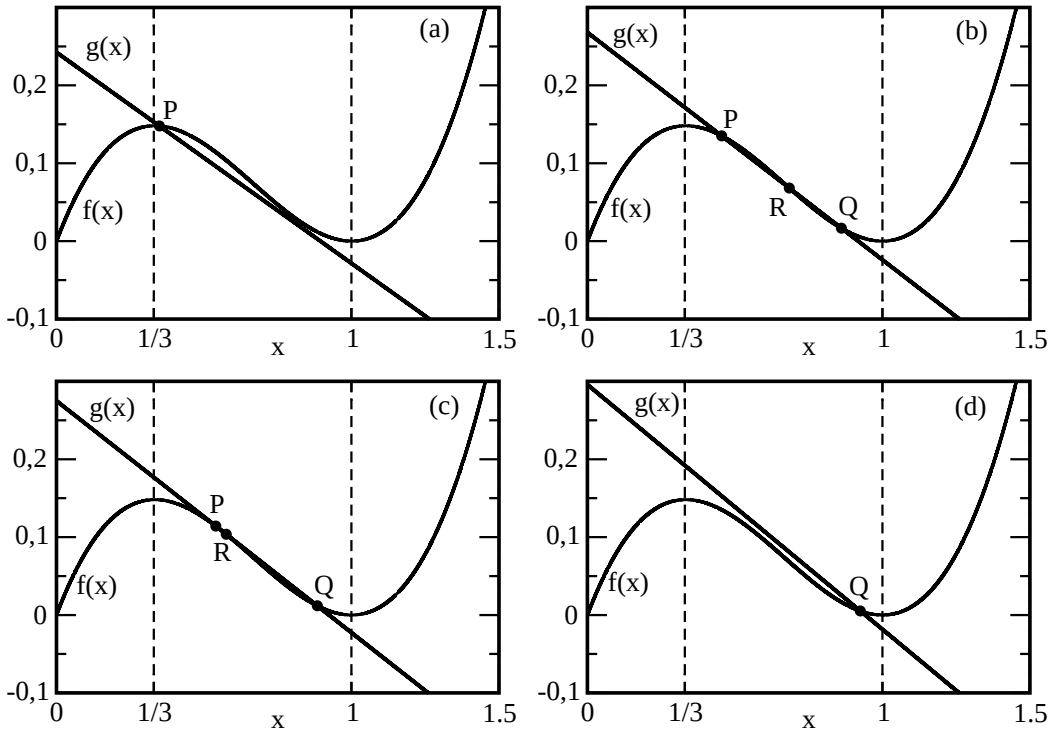

Figure 1: Graphical resolution of Eq. (5) for different values of the driving frequency: $\omega_d = 0.902\ Hz$ (a); $\omega_d = 0.9056\ Hz$ (b); $\omega_d = 0.9065\ Hz$ (c); $\omega_d = 0.909\ Hz$ (d). (The rest of parameters are: $\omega_0 = 1.\ Hz$, $\beta = 3.1 \times 10^{-2}\ s^{-2}$, $\gamma = 5.1 \times 10^{-2}\ s^{-1}$, and $E = 2.4 \times 10^{-1}\ s^{-2}$. This set of parameters is used in all the Figures.)

The system can present monostable or bistable character depending on the combinations of parameters incorporated into the coefficients c_1, c_2. (Following the experimental scheme, in the considered cases, only the driving frequency is varied; the rest of parameters are fixed.) Fig. 1a represents a situation where there is only one attractor, i.e., one stable solution, (the point P). As the frequency is increased, a setting similar to that considered in the experiments emerges. Namely, as shown in Fig. 1b, the system presents then three fixed points: two attractors, (the points P and Q), and one unstable solution, (the point R.) The corresponding basins of attraction are depicted in Fig. 2. [An effective phase space (q, p) has been standardly defined for the coarse-grained scenario by taking $q = A\cos\Psi$, and $p = A\sin\Psi$.] Depending on the initial conditions, the system eventually reaches one or other stable point. For the considered set of parameters, the basins have similar sizes. Hence, a uniform initial distribution of population in the phase space eventually evolves into an approximately symmetric bistable distribution in the attracting sites. Fig. 1c, shows that P comes near to R as the external frequency is increased. As observed in Fig. 1d, further growth of ω_d induces the disappearance of P after converging on the unstable point. (It must be taken into account that the limit of the stability region is reached when the equation $\Delta^2(x_s - 1)(1 - 3x_s) - \gamma^2 = 0$ is fulfilled.)

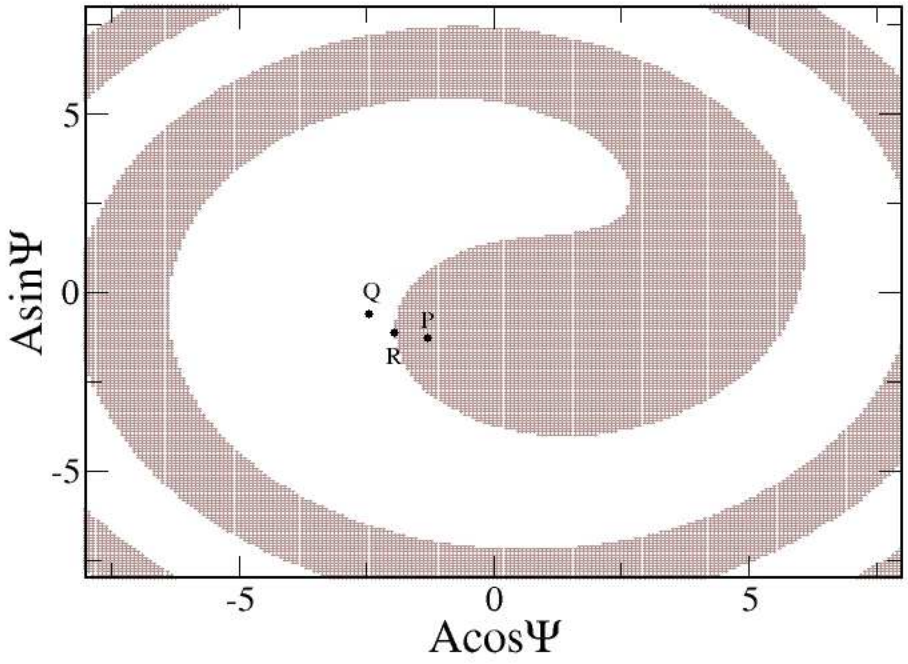

Figure 2: Effective phase space of the averaged system. P and Q denote (stable) attractors, and R represents an unstable solution. The set of parameters is the same as in Fig. 1b. (Arbitrary units are used for the amplitude.)

Closely related to the above analysis is a nontrivial characteristic of the original system. Namely, as reported in [11], the system presents hysteresis in the *evolution* of the stationary amplitudes as the external frequency is varied. Specifically, the stationary values of the amplitude corresponding to an adiabatic sequence of increasing driving frequencies differ from those corresponding to the inverse (frequency-decreasing) sequence. Fig. 3 shows that this aspect of the dynamics is satisfactorily reproduced in the averaged scenario. There, the arrows indicate the *paths* followed by the amplitude as the frequency is increased (or decreased.) The *jumps* in amplitude correspond to the appearance (or disappearance) of the stable fixed points. (Note that as we are focusing on the jumps, and, consequently, have linearized the dynamics around the attractors, our approach does not account for the curbing effect of the nonlinear terms on the amplitude increase.)

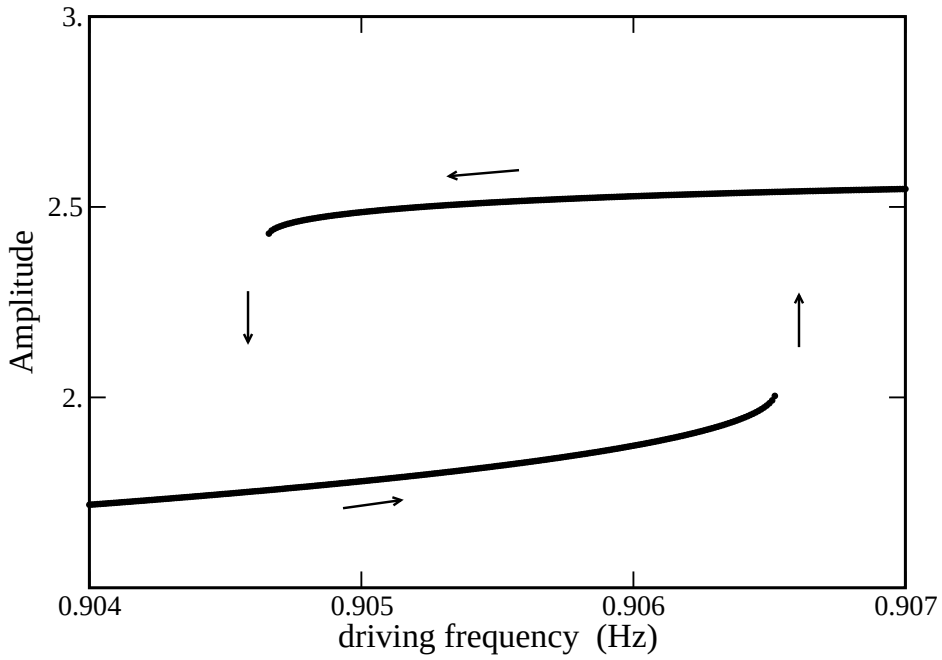

Figure 3: The amplitude (in arbitrary units) of the system response as a function of the external frequency. The parameters are the same as those used in Figs. 1a-1c.

Our description also allows us to connect the appearance of prominent dynamical features with specific locations of the fixed points. It is worth emphasizing the *singular* character of the points characterized by $x_s = 1$ or $x_s = 1/3$. In them, as can be seen from Eqs. (7), (8), and (9), one of the equations becomes autonomous, the corresponding variable entering the other equation as an effective driving. For those solutions, there is only one (real) characteristic frequency, which, as shown by Eq. (10), matches the friction coefficient. Hence, the averaged system, described in terms of $u(t)$ and $v(t)$, is purely dissipative. Correspondingly, the original (unaveraged) set $[z(t), \dot{z}(t)]$ displays damped oscillations with friction coefficient γ at the frequency ω_d. Particularly relevant to the analysis of the spectral peaks in the noisy system is the region defined by $1/3 \leq x_s \leq 1$. In that whole range, (explicitly indicated in Fig. 1), the frequencies $\Omega_\pm$ take real values, as can be seen from Eq. (10). Then, the response of the original system to the driving contains only the frequency ω_d. Moreover, inside that region, an appropriate variation of ω_d can lead one of the attractors to come closer to the unstable solution; in that process, the limit $\Delta^2(x_s - 1)(1 - 3x_s) - \gamma^2 \to 0$ is approached, and, eventually, reached at the unstable point. In contrast, for $x_s < 1/3$ or $x_s > 1$, since the frequencies $\Omega_\pm$ are complex, the primary-system output incorporates, as

components, damped oscillations at frequencies displaced from ω_d. The partial persistence of this differential behavior in the noisy dynamics will be linked to the detected emergence of the supernarrow spectral peaks at ω_d: we will see that it is inside the domain of parameters corresponding to $1/3 \leq x_s \leq 1$ where those peaks appear.

III. THE RESPONSE TO NOISE

Depending on the magnitude of the fluctuations, the stochastic dynamics can significantly differ from the deterministic picture. For instance, for the case of bistable behavior, the system is not longer stabilized in one of the attractors when noise sufficiently intense is added. Instead, it can switch between the basins, the transition rate being a function of the noise strength. This is particularly evident in Fig. 4a, which parallels the noiseless case represented in Figs. 1b and 2. There, we depict a typical random trajectory which displays different flips between the two basins. Still, traces of the crucial role played by the driving frequency in the deterministic dynamics can be observed in the stochastic evolution. An illustrative example is presented in Fig. 4b, which corresponds to the parameters of Fig. 1c, i.e., to a frequency value that reduces the distance between the fixed points P and R. There, it is shown that, as P comes closer to R, the basins are deformed, and a preferential direction for the noise-induced switching becomes patent. In turn, an observable asymmetric partition develops in the stationary distribution of populations. In general, the dynamics can be quite complex: the system can display qualitatively different behaviors depending on the set of parameters. Here, instead of presenting an exhaustive description of the variety of possible outputs, we concentrate on gaining insight into the coherent response to the driving, i.e., into the presence of distinctively sharp peaks in the spectrum. To this aim, it is convenient to start by considering a regime where an analytical description is feasible. Accordingly, in the following, we will extract some clues to basic aspects of the dynamics from the study of a linear version of the model.

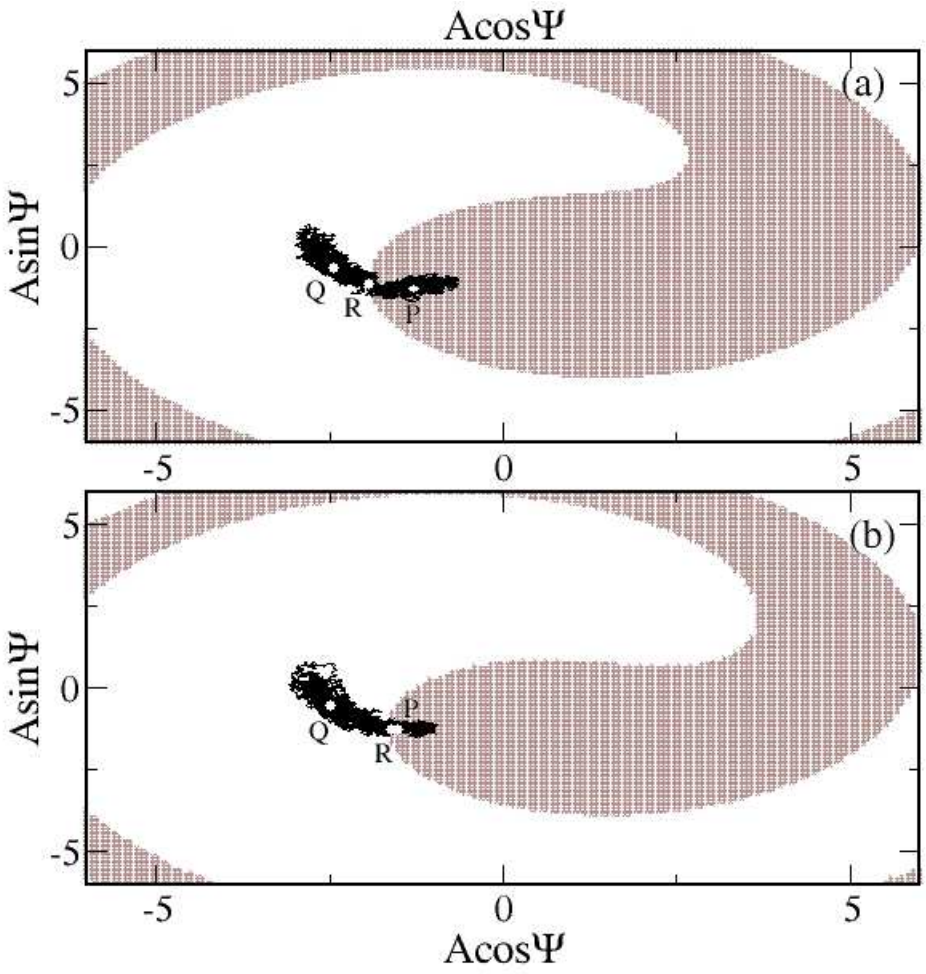

Figure 4: Noisy trajectories in the effective phase space for the set of parameters used in Fig. 1b (a); and for the set of parameters used in Fig. 1c (b). In both cases, the same noise intensity (in arbitrary units) has been used.

A. Analytical approximation to the spectral density

The stochastic linearized equations are given by

$$\dot{u} = -\eta_1 u + \lambda_1 v + \xi_1(t), \tag{16}$$

$$\dot{v} = \lambda_2 u - \eta_2 v + \xi_2(t), \tag{17}$$

where the diagonal and coupling coefficients take the same values as in the noiseless case. (The *deterministic* term $\frac{1}{4}\frac{D_{eff}}{\omega_d}\frac{1}{A}$, present in Eq. (3), does not enter the linearized equations

since it has the same order of magnitude as the neglected quadratic terms in u and v. Its role in the dynamics, relevant for increasing noise intensities, will be discussed later on.) As in the deterministic version, the cases of having $x_s = 1$, (or $x_s = 1/3$), and, in turn, $\lambda_1 = 0$, (or $\lambda_2 = 0$), correspond to *singular* behavior: one of the equations represents then an autonomous Ornstein-Uhlenbeck process [16], which enters the other equation as an additive random term.

To obtain the spectra, we first write the evolution of the position coordinate of the oscillator using the different changes of variables and approximations incorporated so far into our description. Namely, we use the stochastic version of Eq. (12) (now, with noisy $u(t)$ and $v(t)$.) Then, following a standard procedure [15], the spectral density $S[z;\omega] \equiv 2\int_{-\infty}^{\infty} e^{i\omega\tau}\,\langle z(t)z(t+\tau)\rangle\, d\tau$ is calculated as

$$S[z;\omega] \;=\; 2\pi A_s\delta(|\omega|-\omega_d) + \frac{(|\omega|-\omega_d-\lambda_1)^2+(|\omega|-\omega_d+\lambda_2)^2+2\eta_1\eta_2}{[\lambda_1\lambda_2-\eta_1\eta_2+(|\omega|-\omega_d)^2]^2+4(|\omega|-\omega_d)^2\eta_1\eta_2}\,\frac{D_{eff}}{2} \tag{18}$$

The δ-component corresponds to the term $A_s\cos(\omega_d t+\Psi_s)$ in Eq. (12), i.e., it represents a purely deterministic output at ω_d; its weight in the spectrum is determined by the amplitude at the corresponding attractor. The second component of $S[z;\omega]$ incorporates the effect of the fluctuations, present in Eq. (12) through $u(t)$ and $v(t)$. We will focus on this second term, since it was in the (continuous) noisy component of the spectrum where the supernarrow peaks were observed. (The δ-component was removed in the procedure followed to analyze the experimental spectra [11].)

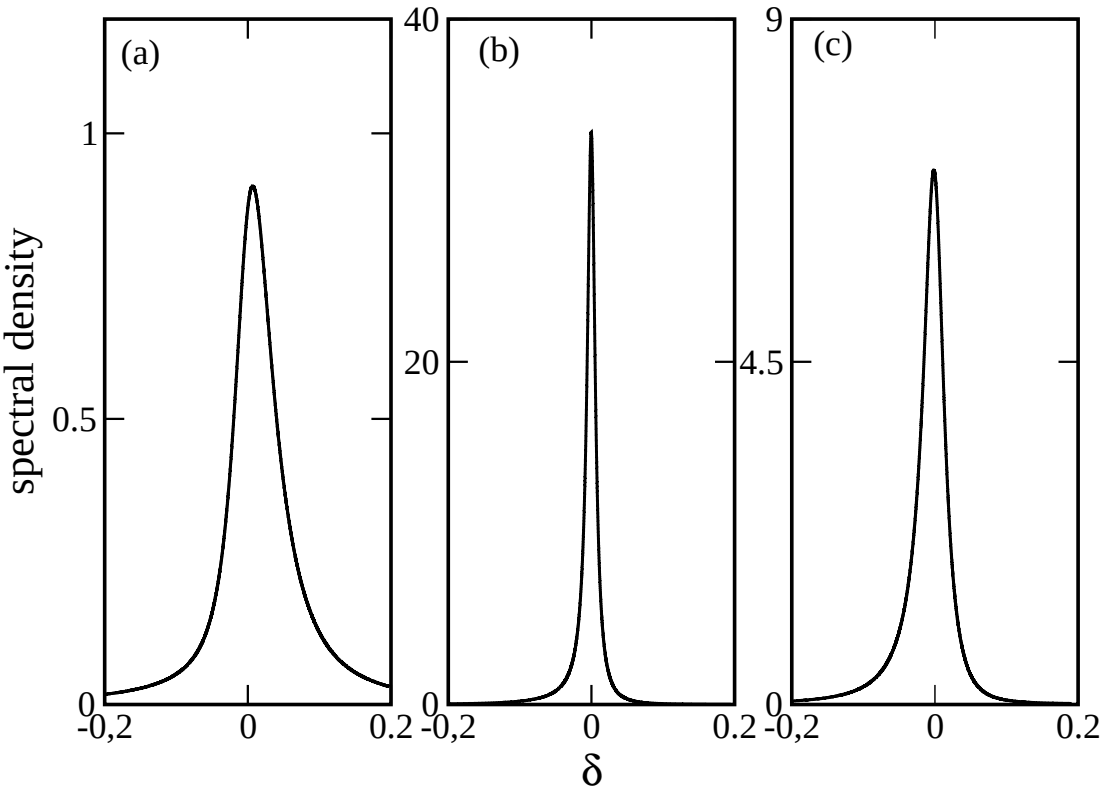

Figure 5: Spectral density (in arbitrary units) as a function of $\delta = \omega - \omega_d$ (in Hz) for three different values of the driving frequency: $\omega_d = 0.902\ Hz$ (a); $\omega_d = 0.9056\ Hz$ (b); and, $\omega_d = 0.909\ Hz$ (c). The rest of parameters are the same as those used in Figs. 1a-1c.

Results for the spectral density obtained from Eq. (18) for three different values of ω_d are represented in Fig. 5. (Note that different vertical scales were used to obtain the graphics.) The connection between the spectral features and the characteristics of the dynamics is established in the following points:

i) As found in the experiments, the spectrum is not symmetric with respect to ω_d. This is apparent in the lack of symmetry of the numerator in Eq. (18), and it is a consequence of the correlation existent between the fluctuations in the amplitude and in the phase, [see Eq. (4).] It is also noticeable in Eq. (18) that, for generic system parameters, the second term in the spectrum does not necessarily peak at ω_d; in fact, more than one peak can be present. The localization and width of those additional peaks change as ω_d is varied. These results, which account for the presence of secondary maxima in the observed spectra, can be understood from our analysis of the noiseless dynamics. It was found that, in a general regime, the deterministic variables $u(t)$ and $v(t)$ can present complex characteristic

frequencies $\Omega_{\pm}$, whose imaginary components imply the occurrence of shifts in the frequency of the complete-system output. Now, we can identify those shifts as leading to spectral peaks displaced from ω_d.

ii) Useful for the characterization of the peaks at ω_d is the introduction of the effective width Γ, defined from Eq. (18) by the expression

$$\Gamma \; = \; \sqrt{|\lambda_1 \lambda_2 - \eta_1 \eta_2|}, \tag{19}$$

which is cast into

$$\Gamma = \sqrt{|\Delta^2 (x_s - 1)(1 - 3x_s) - \gamma^2|} \tag{20}$$

for our particular system. The coherent response to the driving force is marked by the occurrence of a small value of Γ. [Since the different parameters that enter Eq. (20) take finite values, it is the combination of them leading to a small Γ that induces the appearance of the supernarrow peaks.] From the form of Γ, closely related to Eq. (10), the relevance of the former analysis of the stability to the current discussion is evident. Indeed, the mechanism responsible for the sharpening of the peaks can be traced from previous arguments. As the frequency is varied, the localization of the fixed points changes. In particular, the region $1/3 \leq x_s \leq 1$ can be entered. In that domain, there is a preferential response of the system at the driving frequency. Moreover, there is a significant reduction in Γ. The limit case of having $\Gamma = 0$, i.e., of working with parameters that fulfill the equation $\Delta^2 (x_s - 1)(1 - 3x_s) - \gamma^2 = 0$, corresponds to the convergence of one of the attractors on the unstable point. Then, the supernarrow peaks are rooted in the peculiar behavior of the noiseless system when the unstable point inside the region $1/3 \leq x_s \leq 1$ is approached. (Here, a comment on the applicability of our description is pertinent. Given that the linearization of the stochastic equations applies to regimes of significant localization around the attractors, and, therefore, to weak noise, the description becomes less valid as the unstable point is approached. Even so, a sound picture of general trends connected to the observed effects is outlined in our framework.)

It is important to take into account that a small increment in ω_d can qualitatively alter the dynamics. For instance, by slightly shifting the frequency, the whole region $1/3 \leq x_s \leq 1$ can be traversed, and, in turn, significant changes in localization and stability can be induced.

(This is apparent in Fig. 1: in the considered region of intersection between the graphics, small changes in the ordinate at the origin and in the slope of $g(x)$ can considerably alter the set of fixed points.) Then, one can understand the abrupt appearing of the supernarrow peaks, detected through the frequency variation, and qualitatively reproduced in Fig. 5. It follows that the practical realization of the supernarrow-peak regime can require considerable precision in fixing ω_d.

Additional support to the above arguments is provided by the analysis of the peak height Q_{ω_d} i.e., the value of the noisy component of $S[z;\omega]$ at ω_d, which is given by

$$Q_{\omega_d} = \frac{\lambda_1^2 + \lambda_2^2 + 2\gamma^2}{\Gamma^4} \frac{D_{eff}}{2}. \tag{21}$$

In Figs. 6a and 6b, we respectively depict Γ and Q_{ω_d} as a function of ω_d. Following the same sequence as in Fig. 1, we start with a regime where there is only one attractor, P. As the frequency is increased, Γ diminishes, and, in turn, the peak height grows. Eventually, the second attractor Q turns up. In the central region where P and Q coexist, a substantial sharpening of the peaks can be observed. Although it is not equal in both attractors, the width reduction is significant in any of them. As ω_d grows further, only the point Q survives, and the associated Γ displays a monotonous growth in the depicted domain of frequencies. The singularities in Q_{ω_d} mark the appearance (or disappearance) of one of the attractors via its convergence on the unstable point. It is in the specific range of frequencies between the two singularities where the coherent response is strongly localized. The form of the graphics in the central domain points to a coherent response at distances from the unstable point sufficiently large to guarantee the stability at weak noise: the widths (heights) of the peaks are small (large) enough to imply coherence in the dynamics. [The crossing points of the graphics provide illustrative examples of this situation: they are distant from the unstable solution and yet present significantly small (large) values of Γ (Q_{ω_d}).] Hence, despite the noise-induced flips between basins, the system can be expected to spend considerable time in regions, near P or Q, where the behavior is coherent.

The presence of approximately equal populations in the attractors, identified in a preliminary analysis of the experimental results as an indicator of the supernarrow-peak regime, can be explained within our approach. In the regime of small Γ, i.e., inside the region $1/3 \leq x_s \leq 1$, the basins have similar sizes, and, consequently, any uniform initial arrangement of population ends up as an approximately symmetric partition between the two

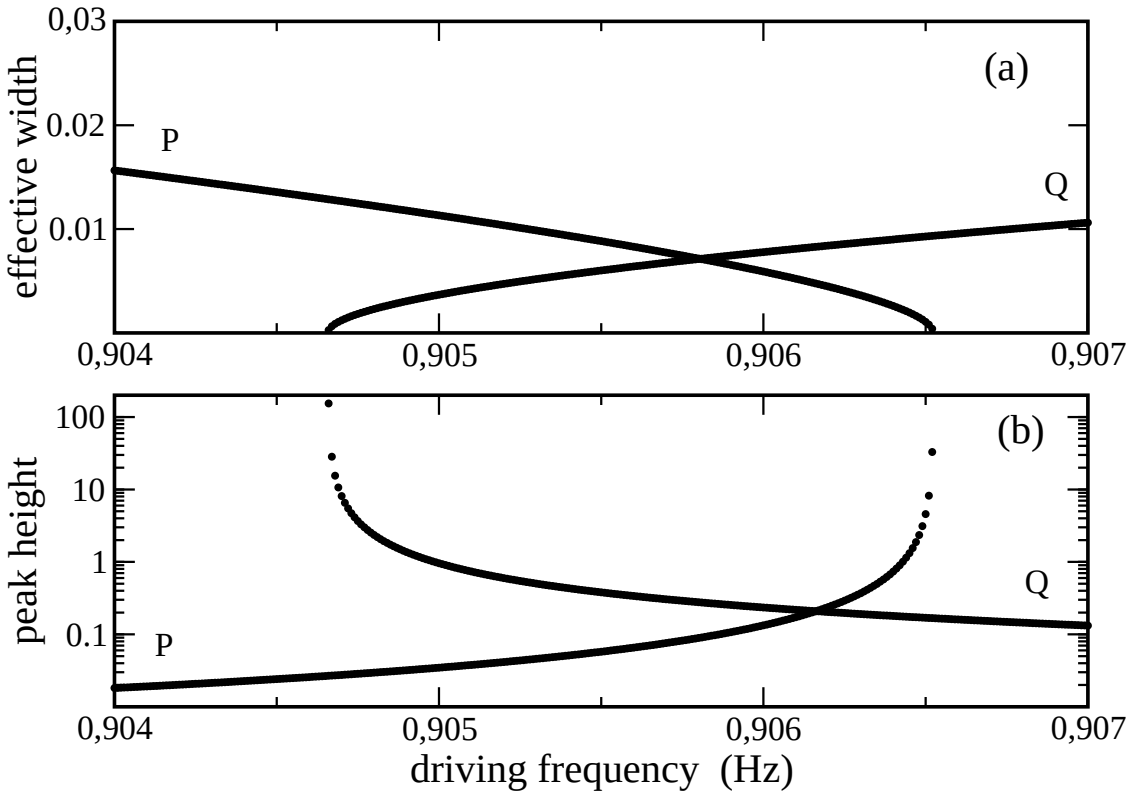

Figure 6: Effective width (a) and height of the spectral peak (b) (both in arbitrary units) as a function of the driving frequency. The parameters are the same as those used in Figs. 1a-1c.

iii) Special care is needed in assessing the persistence of the supernarrow spectral peaks as the magnitude of the fluctuations is enhanced. For a growing noise intensity, the rate of switching between the basins increases, and the dependence of the spectral density on the effective noise strength D_{eff} becomes nontrivial. (Recall that the spectral density given by Eq. (18) is strictly valid in the considered weak-noise limit.) For stronger fluctuations, apart from an increasing number of noise-induced transitions, the system develops a less coherent behavior inside each basin. As a result, the peaks broaden. Some insight into this behavior is obtained from the analysis of the role of the noise-induced *deterministic* term $\frac{1}{4}\frac{D_{eff}}{\omega_d}\frac{1}{A}$ present in Eq. (3) and of the strictly random component of Eq. (4), $\frac{\xi_2(t)}{A}$. Both terms have a stronger effect as the localization of the fixed points approaches smaller amplitudes. (An implication related to this noise-induced *asymmetry* is that the *noisy* trajectories do not reach the point with $A = 0$.) The term $\frac{1}{4}\frac{D_{eff}}{\omega_d}\frac{1}{A}$ modifies the position of the fixed points obtained from

the purely deterministic picture. From a scenario of extended applicability of the linearized equations, this term can be reasonably conjectured to change also the parameters that determine the effective width of the peaks in the spectrum, and, consequently, to prevent reaching small values of Γ. Additionally, the multiplicative character of the random term can significantly affect the form of the spectral density. Then, although our approach does not describe the transitions between attracting sites, it is primarily understood from it that, as the noise intensity grows, the coherence in the response to the driving decays. Still, given the robust character of their deterministic roots, i.e., of the peculiar dynamics near each of the attractors, the peaks can be expected to be observable for moderate noise intensities.

B. General aspects of the supernarrow-peak regime

We turn now to evaluate the generality of the considered effects. From the above analysis, a procedure to identify similar features in other driven systems can be established. Moreover, the criteria for their emergence can be defined. We consider a *generic* system, where, as preliminary requirements, it is assumed that a coarse-grained reduction is feasible and that a linearization of the resulting effective stochastic equations applies. Hence, we deal with a system described by Eqs. (16) and (17) with general coefficients η_i and λ_i, $(i = 1, 2)$. From the following arguments, sufficient conditions for the appearance of the supernarrow peaks are set up:

First, given that the linearization method implies a restriction of the dynamics to the areas around the fixed points, the stability requirements, given by Eqs. (13) and (14), must hold. Second, since a preferential output of the system at the driving frequency is intended, we must look for characteristic frequencies of the averaged system which take real values. (This corresponds to have only the frequency ω_d in the original-system response.) From Eq. (10), it is apparent that the frequencies $\Omega_\pm$ are real when the inequality $(\eta_1 - \eta_2)^2 + 4\lambda_1\lambda_2 > 0$ holds. A final requirement comes from imposing a reduced width for the spectral peaks. Namely, a small value of $\Gamma = \sqrt{|\lambda_1\lambda_2 - \eta_1\eta_2|}$ is needed to guarantee the sharpening of the spectral peaks.

This procedure implies the control of the elements of the system which are essential for the appearance of a coherent response to the driving. The resulting set of restrictions defines the aimed range of parameters. (Corrections to the simplified picture given by our approach

must be implemented when the system presents a highly-nonlinear term or incorporates strong fluctuations.)

It is worth mentioning that an additional element of generality is provided by the compact characterization of the nonlinear oscillator specifically considered in our study: the coefficients c_1 and c_2 embody all the influence of the system elements on the analyzed effects. This compact character facilitates setting up a common framework for the analysis of different systems. (Examples can be found in [15].)

IV. CONCLUDING REMARKS

Our approximate description of the stochastic dynamics of a damped and driven nonlinear oscillator has allowed us to establish a link between the appearance of distinctively supernarrow peaks in the spectrum and specific aspects of the deterministic dynamics. Although the preferential response at the driving frequency, marked by the appearance of supernarrow spectral peaks, occurs in the domain of bistability, it is the dynamics near each attracting site that accounts for the observed coherence. The peaks have been shown to become more prominent when, with the system still inside the stability domain, one the attractors approaches the unstable solution. One significant implication of these findings is that, for those features to persist when the noise intensity is increased, significant permanence in the stability region must be guaranteed. Actually, the coherent response seems to be robust against the dephasing effects of the noise-induced transitions between basins: the deterministic roots of the effect are still patent for growing noise strength.

We stress that despite the use of scaled parameters (convenient for the calculations) and of different approximations, the analysis reproduces the main features detected in the experiments. Namely, the hysteresis curve for the amplitude versus the frequency, the form of the spectral densities, and the similar values of the populations in the attractors in the supernarrow regime are satisfactorily simulated.

The supernarrow spectral peaks have been reproduced with a model where the noise correlation-time has been considered to be much smaller than any other time scale in the system. In fact, this is a requirement for the validity of the stochastic version of the applied averaging method. Hence, there are no qualitative differences between the broadband regime, considered in our approach, (and realized in the experiments), and the strict white-noise

limit. The analysis of the role of specific colored-noise characteristics requires going beyond the used coarse-grained approach.

The study uncovers the generality of the mechanism behind the observed effects, and, therefore, its relevance to different contexts. The compact character of our description facilitates the possibility of controlling the setup, in particular, of varying the components to systematically characterize the response under well-defined conditions. The realization of similar effects in unexplored regimes is then open.

---

[1] F. Moss and P. V. E. McClintock, Noise in Nonlinear Dynamical Systems, 1st ed. (Cambridge University Press, Cambridge, UK, 2007), Vols. 1 and 2.

[2] L. Gammaitoni, P. Hänggi, P. Jung and F. Marchesoni, Rev. Mod. Phys. **70**, 223 (1998).

[3] P. S. Landa and P. V. E. McClintock, Phys. Rep. **323**, 4 (2000).

[4] L. J. Lapidus *et al.*, Phys. Rev. Lett. **83**, 899 (1999).

[5] M. I. Dykman *et al.*, Phys. Rev. E **57**, 5202 (1998).

[6] S. Brouard and J. Plata, Phys. Rev. A **83**, 063408 (2011).

[7] A. Pikovsky, M. Rosenblum, J. Kurths, Synchronization: A Universal Concept in Nonlinear Sciences, Cambridge University Press, Cambridge, 2001.

[8] B. Lindner, J. García-Ojalvo, A. Neiman, and L. Schimansky-Geier, Phys. Rep. **392**, 321 (2004).

[9] L. G. Villanueva, E. Kenig, R. B. Karabalin, M. H. Matheny, Ron Lifshitz, M. C. Cross, and M. L. Roukes, Phys. Rev. Lett. **110**, 177208 (2013).

[10] Eyal Kenig, M. C. Cross, Ron Lifshitz, R. B. Karabalin, L. G. Villanueva, M. H. Matheny, and M. L. Roukes, Phys. Rev. Lett. **108**, 264102 (2012).

[11] C. Stambaugh and H. B. Chan, Phys. Rev. Lett. **97**, 110602 (2006).

[12] M. I. Dykman *et al.*, Phys. Rev. Lett. **65**, 48 (1990)

[13] M. I. Dykman and Krivoglaz, Sov. Phys. JETP **50**, 30 (1979)

[14] N. N. Bogoliubov and Y. A. Mitropolsky, *Asymptotic Methods in the Theory of Non-Linear Oscillations* (Gordon and Breach, New York, 1961).

[15] R. L. Stratonovich, *Topics in the Theory of Random Noise* (Gordon and Breach, New York, 1963).

[16] H. Risken, *The Fokker-Planck Equation* (Springer-Verlag, New York, 1989)

[17] J. Plata, Phys. Rev. E **59**, 2439 (1999).

[18] R. Lifshitz and M.C. Cross in *Reviews of Nonlinear Dynamics and Complexity*, edited by por Heinz Georg Schuster, (Wiley, Weinheim, 2008).